JOC Article

Methyl Substitutent Effects in Radical Cation Diels−Alder Reactions

Nicholas A. Valley and Olaf Wiest*

Department of Chemistry and Biochemistry, University of Notre Dame, Notre Dame, Indiana 46556-5670

owiest@nd.edu

Received October 2, 2006

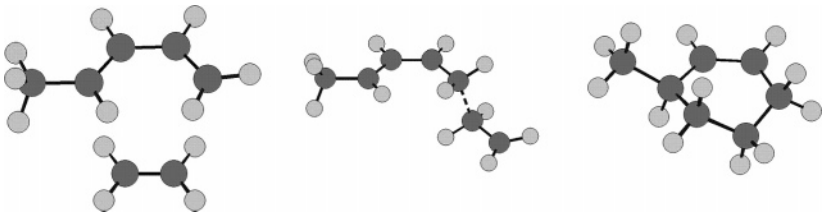

The effect of methyl substitution on the Diels−Alder radical cation reaction was studied using B3LYP with a 6-31G* basis set. Five separate pathways, one concerted and four stepwise, were examined for each possible position of a methyl substituent. None of the concerted transition structures could be located without symmetry constraints, and all but one of the structures obtained under these conditions were destabilized by a second-order Jahn−Teller distortion. A concerted pathway with simultaneous bond formation at C1 and C4 is therefore excluded. Stepwise pathways that had the methyl group either on a carbon involved in the initial bond formation or in a position where it could not stabilize the radical/cation were a few kcal/mol above alternate pathways. High transition state energies for the formation of vinylcyclobutane derivatives cause it to be a minor product in general. The pathway that proceeds through an anti-intermediate is the most favored, while the pathways forming the gauche-out intermediate that converts to the anti-intermediate is also strongly represented. Both of the major pathways lead directly to the formation of the methylcyclohexene product.

Introduction

The Diels−Alder reaction is an important synthetic tool, allowing the easy and selective formation of six-membered rings. In most cases, different electron densities of the diene and dienophile starting materials are necessary to lower the activation barrier and achieve practical reaction rates. One possibility to circumvent this requirement is the electron-transfer-catalyzed Diels−Alder reaction,[1] where one of the reactants is oxidized to the radical cation,[2] which then rapidly undergoes cycloadditions to form the product radical cation. After back electron transfer, the final product is formed at overall rates many orders of magnitudes faster than the corresponding uncatalyzed reaction.[3] At the same time, the radical cation version has been shown experimentally to have very high regio- and diastereoselectivity.[4] To fully utilize the synthetic potential of these reactions, it would be desirable to know the mechanistic pathway(s) that are available and understand what effect substitutions have on determining the favored pathway, on rates, and on the selectivity of the reaction.

The first of these necessities has been covered by multiple computational studies of the parent reaction from our laboratory[5]

(1) For overviews, see, for example: (a) Bauld, N. L. *Tetrahedron* **1989**, *45*, 5307−5363. (b) Chanon, M.; Eberson, L. In *Photoinduced Electron Transfer Part A*; Chanon, M., Fox, M. A., Eds.; Elsevier: Amsterdam, 1989; pp 409−597. (c) Bauld, N. L. In *Advances in Electron Transfer Chemistry Vol. 2*; Mariano, P. S., Ed.; JAI Press: New York, 1992; pp 1−66. (d) Mattay, J. *Synthesis* **1989**, 233−252. (e) Schmittel, M.; Burghart, A. *Angew. Chem., Int. Ed. Engl.* **1997**, *36*, 2551−2589. (f) Pandey, G. *Top. Curr. Chem.* **1993**, *168*, 175−221.

(2) Although the pericyclic reactions of radical anions, formed through reductive electron transfer, are in principle possible, there are few examples described in the literature. (a) Arnold, D. R.; Maroulis, A. J. *J. Am. Chem. Soc.* **1977**, *99*, 7355−7356. (b) Fox, M. A.; Hust, J. R. *J. Am. Chem. Soc.* **1984**, *106*, 7626−7627. (c) Yang, J.; Cauble, D. F.; Berro, A. J.; Bauld, N. L.; Krische, M. J. *J. Org. Chem.* **2004**, *69*, 7979−7984. (d) Felton, G. A. Bauld, N. L. *Tetrahedron* **2005**, *61*, 3515−3523.

(3) This possibility for catalysis of the Diels−Alder reaction was first proposed more than 60 years ago: Woodward, R. B. *J. Am. Chem. Soc.* **1942**, *64*, 3058−3059.

(4) For example: (a) Harirchian, B.; Bauld, N. L. *J. Am. Chem. Soc.* **1989**, *111*, 1826−1828. (b) Gieseler, A.; Steckhan, E.; Wiest, O.; Knoch, F. *J. Org. Chem.* **1991**, *56*, 1405−1411.

(5) (a) Haberl, U.; Steckhan, E.; Wiest, O. *J. Am. Chem. Soc.* **1999**, *121*, 6730−6736. (b) Haberl, U.; Steckhan, E.; Wiest, O.; Blechert, S. *Chem.-Eur. J.* **1999**, *5*, 2859−2865.

10.1021/jo0620361 CCC: $37.00
Published on Web 12/23/2006

SCHEME 1. Pathways of the Diels−Alder Radical Cation Reaction

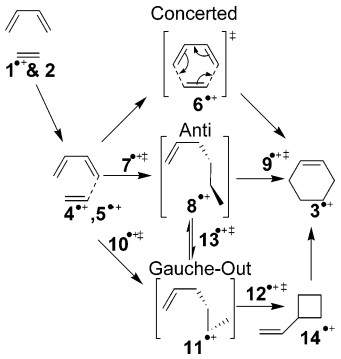

and others.[6] The different possible pathways for the reaction of the butadiene radical cation and ethylene or acetylene were mapped out. These studies identified the pathways shown in Scheme 1, which closely resemble the corresponding structures in the biradical, stepwise reaction.[7] Systematic studies of substituent effects on radical cation reactions are much rarer. While there are some experimental studies of substituent effects on reactivity and regioselectivity,[8] these studies can by necessity not provide insights at the atomic level or about pathways that are higher in energy by more than a few kcal/mol. There are also a limited number of computational studies involving more complicated starting materials,[9] such as the reaction of indoles with cyclic or highly substituted dienes. However, there is to the best of our knowledge only a single systematic study of substituent effects in radical ion chemistry[10] and no attempts to systematically probe the effects of a substituent on the different positions in the bimolecular radical cation Diels−Alder reaction.

The overall mechanistic scheme for the Diels−Alder radical cation reaction that emerged from the previous studies of the parent system[6] is shown in Scheme 1. There are five different possible pathways that can be taken to form the cyclohexene radical cation **3**$^{\bullet+}$. First, there is the concerted pathway, which has been shown to be subject to a second-order Jahn−Teller distortion in its transition state **6**$^{\bullet+}$ leading to one of the other, stepwise pathways. The concerted pathway was therefore not considered to be a viable mechanism.[6] As mentioned before, the four other pathways are similar to the diradical pathways of the neutral reaction. One involves an initial bond formation in an anti conformation to form intermediate **8**$^{\bullet+}$, which then closes down to cyclohexene, while another forms the bond in a gauche-out fashion via intermediate **11**$^{\bullet+}$, which then closes to vinylcyclobutane **14**$^{\bullet+}$ before finally rearranging to **3**$^{\bullet+}$. This "indirect Diels−Alder reaction" has been experimentally observed in a number of heterosubstituted systems.[11] These two stepwise pathways are connected via the anti and gauche-out intermediates by a rotation around the previously formed bond, bringing the total number of possible pathways to five.

The previously studied parent system does not provide any information into the origins of regiochemistry or the effects of desymmetrization of the substrates on the reaction pathways. To study these effects, a single methyl group was placed in each possible position of each structure in the mechanistic scheme, and properties of optimized structures were compared to reveal the effect of substitution. The computational studies completed in this work provide a starting point to decipher how different patterns of substitution will affect the choice of mechanism and therefore the final products that form. By systematically studying the effect a single methyl substituent has on the energies of the structures in each pathway, the magnitude and type of stabilization or destabilization can be reasoned. This will form a basis for future studies and predictions of selectivity for more complicated systems.

Computational Methodology

All transition structures and intermediate structures in the reaction scheme were optimized at the B3LYP/6-31G* level of theory with Gaussian 03.[12] All reported charges were calculated with ChelpG. This level of theory has shown to be reliable in terms of energy differences when compared to computationally much more expensive highly correlated MO methods.[13] Harmonic frequency analysis confirmed that intermediate structures corresponded to minima and transition states had a single imaginary frequency except in cases discussed in more detail in the text. Imaginary frequencies were visualized using GaussView 3.09 to confirm the correct transition vector was being followed. Starting geometries were obtained from earlier studies on the parent radical cation Diels−Alder reaction.[5] All energies are corrected for zero-point energies and are reported in kcal/mol relative to the product formed in each case. In cases where no stationary point could be located, scans of the appropriate internal coordinate were performed to either locate a better starting

(6) (a) Hofmann, M.; Schaefer, H. F. *J. Am. Chem. Soc.* **1999**, *121*, 6719−6729. (b) Hofmann, M.; Schaefer, H. F. *J. Phys. Chem. A* **1999**, *103*, 8895−8905. (c) Hu, H.; Wenthold, P. G. *J. Phys. Chem. A* **2002**, *106*, 10550−10553. (d) Goebbert, D. J.; Liu, X.; Wenthold, P. G. *J. Am. Soc. Mass Spectrom.* **2004**, *15*, 114−120. (e) van der Hart, W. J. *Int. J. Mass Spectrom.* **2001**, *208*, 119−125. (f) Bouchoux, G.; Salpin, J.-Y.; Yanez, M. *J. Phys. Chem. A* **2004**, *108*, 9853−9862. (g) Bouchoux, G.; Nguyen, M. T.; Salpin, J.-Y. *J. Phys. Chem. A* **2000**, *104*, 5778−5786. (h) Bauld, N. L. *J. Am. Chem. Soc.* **1992**, *114*, 6800−5804. (i) Bellville, D. J.; Bauld, N. L. *Tetrahedron* **1986**, *42*, 6167−6173.

(7) (a) Goldstein, E.; Beno, B.; Houk, K. N. *J. Am. Chem. Soc.* **1996**, *118*, 6036−6043. For a more detailed discussion of the relationship between the diradical and radical cationic pathways, see: (b) Donoghue, P.; Wiest, O. *Chem.-Eur. J.* **2006**, *12*, 7018−7026. (c) Saettel, N. J.; Oxgaard, J.; Wiest, O. *Eur. J. Org. Chem.* **2001**, 1429−1439.

(8) Martiny, M.; Steckhan, E.; Esch, T. *Chem. Ber./Recl.* **1993**, *126*, 1671−1682.

(9) (a) Wiest, O.; Steckhan, E.; Grein, F. *J. Org. Chem.* **1992**, *57*, 4034−4037. (b) Saettel, N. J.; Wiest, O.; Singleton, D. A.; Meyer, M. P. *J. Am. Chem. Soc.* **2002**, *124*, 11552−11559. (c) Ferreiro, M. L.; Rodriguez-Otero, J.; Cabaleiro-Lago, E. M. *Struct. Chem.* **2004**, *15*, 323−326. (d) Furmeier, S.; Metzger, J. O. *J. Am. Chem. Soc.* **2004**, *126*, 14485−14492.

(10) Swinarski, D. J.; Wiest, O. *J. Org. Chem.* **2000**, *65*, 6708−6714.

(11) (a) Pabon, R. A.; Bellville, D. J.; Bauld, N. L. *J. Am. Chem. Soc.* **1984**, *106*, 2730−2731. (b) Reynolds, D. W.; Harirchian, B.; Chiou, H.; Marsh, B. K.; Bauld, N. L. *J. Phys. Org. Chem.* **1989**, *2*, 57−88. (c) Botzem, J.; Haberl, U.; Steckhan, E.; Blechert, S. *Acta Chem. Scand.* **1998**, *52*, 175−193.

(12) Frisch, M. J.; Trucks, G. W.; Schlegel, H. B.; Scuseria, G. E.; Robb, M. A.; Cheeseman, J. R.; Montgomery, J. A., Jr.; Vreven, T.; Kudin, K. N.; Burant, J. C.; Millam, J. M.; Iyengar, S. S.; Tomasi, J.; Barone, V.; Mennucci, B.; Cossi, M.; Scalmani, G.; Rega, N.; Petersson, G. A.; Nakatsuji, H.; Hada, M.; Ehara, M.; Toyota, K.; Fukuda, R.; Hasegawa, J.; Ishida, M.; Nakajima, T.; Honda, Y.; Kitao, O.; Nakai, H.; Klene, M.; Li, X.; Knox, J. E.; Hratchian, H. P.; Cross, J. B.; Bakken, V.; Adamo, C.; Jaramillo, J.; Gomperts, R.; Stratmann, R. E.; Yazyev, O.; Austin, A. J.; Cammi, R.; Pomelli, C.; Ochterski, J. W.; Ayala, P. Y.; Morokuma, K.; Voth, G. A.; Salvador, P.; Dannenberg, J. J.; Zakrzewski, V. G.; Dapprich, S.; Daniels, A. D.; Strain, M. C.; Farkas, O.; Malick, D. K.; Rabuck, A. D.; Raghavachari, K.; Foresman, J. B.; Ortiz, J. V.; Cui, Q.; Baboul, A. G.; Clifford, S.; Cioslowski, J.; Stefanov, B. B.; Liu, G.; Liashenko, A.; Piskorz, P.; Komaromi, I.; Martin, R. L.; Fox, D. J.; Keith, T.; Al-Laham, M. A.; Peng, C. Y.; Nanayakkara, A.; Challacombe, M.; Gill, P. M. W.; Johnson, B.; Chen, W.; Wong, M. W.; Gonzalez, C.; Pople, J. A. *Gaussian 03*, revision C.02; Gaussian, Inc.: Wallingford, CT, 2004.

(13) (a) Wiest, O. *J. Am. Chem. Soc.* **1997**, *119*, 7513−7519. (b) Oxgaard, J.; Wiest, O. *J. Am. Chem. Soc.* **1999**, *121*, 11531−11537. (c) Sastry, G. N.; Bally, T.; Hrouda, V.; Carsky, P. *J. Am. Chem. Soc.* **1998**, *120*, 9323−9334. (d) Hrouda, V.; Carsky, P.; Ingr, M.; Chval, Z.; Sastry, G. N.; Bally, T. *J. Phys. Chem. A* **1998**, *102*, 9297−9307.

SCHEME 2. Substituent Patterns Investigated

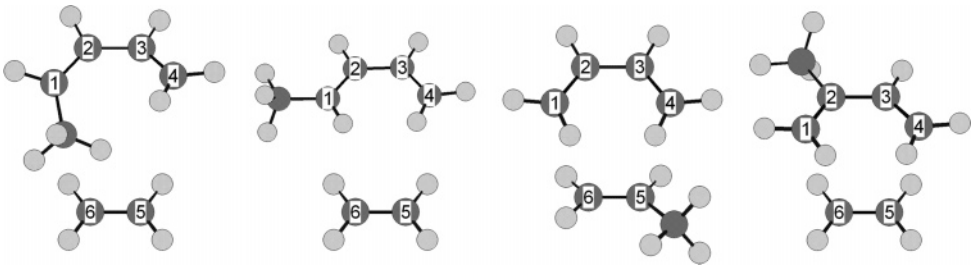

geometry of the stationary point or confirm its absence. Plots of these scans are included in the Supporting Information.

The structures are named according to the position of the methyl group in the starting material, the carbon atoms the initial bond forms between, and which intermediate or transition state it corresponds to in Scheme 1. Position 1 refers to the reaction of *cis*-1,3-pentadiene and ethylene, position 2 to *trans*-1,3-pentadiene and ethylene, position 3 to 1,3-butadiene and 1-propylene, and position 4 to 2-methyl-1,3-butadiene and ethylene. These four combinations are shown in Scheme 2 along with the numbering of the carbons in each case. For three of the positions, the initial bond can be formed to either C1 (denoted with an **a** after the position number) or to C4 (denoted with a **b**). Position 3 is also named with an **a** for bond formation to C5 and a **b** for C6, but an **x** or **e** is also added depending on whether the bond formed with the methyl group pointing in the exo or endo position, respectively.

Results and Discussion

Position 1: *cis*-1,3-Pentadiene and Ethylene. For the reaction of *cis*-1,3-pentadiene and ethylene, the initial bond in the stepwise pathways can be formed to C1, the carbon attached to the methyl group, or at C4, the unsubstituted terminal carbon, corresponding to pathways a and b, respectively. The fully separated starting materials $\mathbf{1}^{\bullet+}+\mathbf{2}$ are 33.7 kcal/mol above the product (3-methyl-1-cyclohexene radical cation). Formation of the ion−molecule complexes $\mathbf{1b-4}^{\bullet+}$ and $\mathbf{1a-4}^{\bullet+}$ is exothermic by 7.2 and 6.4 kcal/mol, respectively. This binding energy of the ion−molecule complexes is approximately 4 kcal/mol less than that calculated for the parent system at the same level of theory, indicating the better stabilization of the radical cation in $\mathbf{1}^{\bullet+}$ by the electron-donating methyl group. The calculated bond lengths of the forming bonds, shown in Figure 1, are 0.2−0.4 Å longer than in the parent case. This, and differences in bond lengths and relative energies between $\mathbf{1b-4}^{\bullet+}$ and $\mathbf{1a-4}^{\bullet+}$, is also consistent with an increased stabilization of the radical cations.

The relative energies of the five different pathways involved in the attack of ethylene on C4 of *cis*-pentene radical cation are shown in Figure 2. The ion−molecule complex for the concerted pathway $\mathbf{1b-5}^{\bullet+}$ has an energy of 28.6 kcal/mol, 2.1 kcal/mol higher in energy than in the parent case. However, no transition structure connecting $\mathbf{1b-5}^{\bullet+}$ directly to the product could be located, and all attempts to do so without constraints resulted in transition structures leading to one of the stepwise pathways described below. In analogy to the previous studies of the reaction,[5,6] the two forming bond lengths C1−C6 and C4−C5 were therefore constrained to be identical. This led to $\mathbf{1b-6}^{\bullet+}$ with a relative energy of 47.5 kcal/mol. It is noteworthy that $\mathbf{1b-6}^{\bullet+}$ is, in analogy to the findings for the parent reaction, a second-order saddle point. This indicates that, despite the fact that the methyl substituent breaks the formal C_s symmetry, the corresponding orbitals are still essentially degenerate and subject to a Jahn−Teller effect. Even though the energy of $\mathbf{1b-6}^{\bullet+}$ is formally an upper limit for a concerted transition structure because of the constraints applied, the concerted pathway is considered to be energetically highly disfavored as compared to the other pathways.

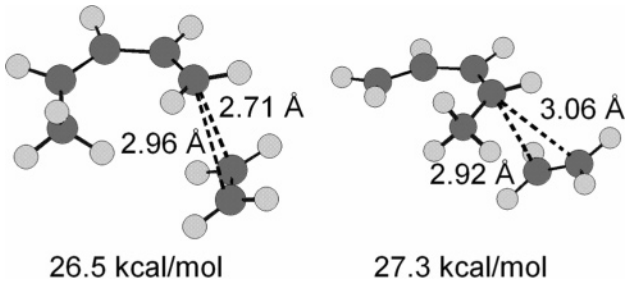

FIGURE 1. Structures and relative energies of ion−molecule complexes $\mathbf{1b-4}^{\bullet+}$ (left) and $\mathbf{1a-4}^{\bullet+}$ (right).

The transition structure for the formation of the first bond between the dienophile and C4 of the diene, $\mathbf{1b-7}^{\bullet+}$, is 1.9 kcal/mol higher than the ion−molecule complex and leads to the anti-intermediate $\mathbf{1b-8}^{\bullet+}$ with a relative energy of 26.3 kcal/mol. In comparison, the energy of the gauche-out transition structure $\mathbf{1b-10}^{\bullet+}$ is 29.4 kcal/mol, leading to the gauche-out intermediate $\mathbf{1b-11}^{\bullet+}$ with a relative energy of 27.7 kcal/mol. Ring closure to the 3-methyl cyclohexene radical cation $\mathbf{1b-3}^{\bullet+}$ and 1-propenyl cyclobutane radical cation $\mathbf{1b-14}^{\bullet+}$ occurs with activation energies of 2.2 and 3 kcal/mol, respectively. This makes, similarly to the unsubstituted case but contrary to the biradical reaction,[7a] the ring-closing step the rate-limiting step in both cases along the reaction pathways of the radical cations. Interestingly, the transition structure for the interconversion between the two pathways, $\mathbf{1b-13}^{\bullet+}$, has essentially the same energy as the transition structure for ring closure to $\mathbf{1b-3}^{\bullet+}$. This is in agreement with the experimental observation that formation of the cyclobutene product is typically not observed in the radical cation Diels−Alder reaction of simple hydrocarbons. While the relative energies of the intermediates involved in the two pathways are very similar to the ones obtained for the parent system,[5,6] the calculated activation energies along the pathways are 1−1.5 kcal/mol higher than in the unsubstituted case.

As already shown in Figure 2, pathway a leading to the other regioisomer $\mathbf{1b-3}^{\bullet+}$ is disfavored in comparison to pathway b (for a complete scheme of the reaction pathway, see the Supporting Information). While the energy difference of 0.8 kcal/mol at the stage of the ion−molecule complex is small, it increases to 6.8 kcal/mol at the stage of the anti-intermediates $\mathbf{1b-8}^{\bullet+}$ and $\mathbf{1a-8}^{\bullet+}$, shown in Figure 3.

In the ion−molecule complexes, which lead to the stepwise pathways, the shortest carbon−carbon bond is 2.92 Å in **1a**−

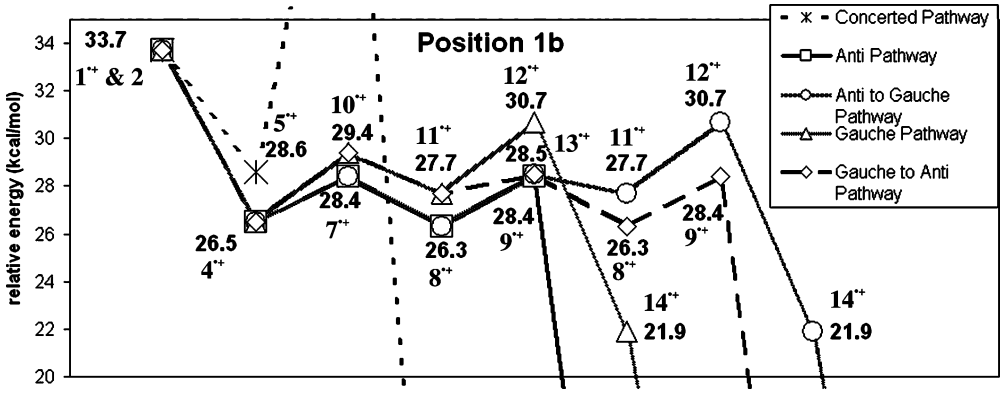

FIGURE 2. Calculated reaction profiles for reaction 1b. Second-order transition structure at 47.5 kcal/mol and 3-methyl cyclohexene product at 0 kcal/mol are not shown.

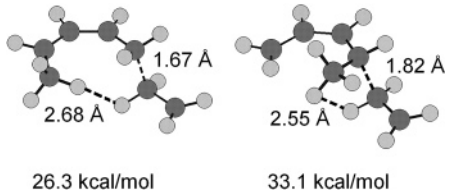

FIGURE 3. Intermediate structures and relative energies of **1b**−**8**•+ and **1a**−**8**•+.

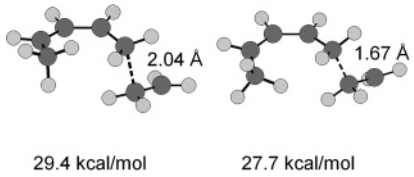

FIGURE 4. Transition structure **1b**−**10**•+, intermediate structure **1b**−**11**•+, and their relative energies.

4•+ and 2.71 Å in **1b**−**4**•+. From this ion−molecule complex, either the anti or the gauche-out intermediate can form. The length of the bond being formed shortens to 1.87 Å in **1a**−**7**•+ and 2.10 Å in **1b**−**7**•+. Figure 3 shows optimized structures of the anti-intermediates formed as the bond length shortens to 1.82 and 1.67 Å for **1a**−**8**•+ and **1b**−**8**•+, respectively. In both structures, a hydrogen atom on the ethylene is near a hydrogen of the methyl group (2.55 Å for **1a**−**8**•+ and 2.68 Å for **1b**−**8**•+).

The transition structure for the formation of the gauche-out intermediate has a C4−C5 bond length of 2.04 Å. A length of 1.67 Å is observed in the gauche-out intermediate structure **1b**−**11**•+ (Figure 4).

Transition structure **1a**−**7**•+ is at 32.9 kcal/mol, which leads to the anti-intermediate **1a**−**8**•+ at 33.1 kcal/mol. Radical cation 1-methyl-2-vinyl-cyclobutane, **1a**−**14**•+, is 29.4 kcal/mol above the cyclohexene product, and the transition structure **1a**−**12**•+ has an energy of 39.2 kcal/mol.

Certain structures, such as **1a**−**10**•+ and **1a**−**11**•+, did not optimize to the desired stationary point. When this occurred, frequencies were calculated at every point of the optimization. If this failed, a scan was completed, optimizing at each point along the reaction coordinate, which changes to get to the desired structure in the reaction scheme. In a few cases, this revealed that the transition was barrierless with the level of theory used. The majority of the time, however, during the scan the structure's geometry and energy would undergo large shifts.

TABLE 1. Charges and Spin Densities (Hydrogens Summed into Heavy Atoms) for Starting Materials and Anti-intermediates in Pathway 1

	1•+**+2**		**1a**−**8**•+		**1b**−**8**•+	
carbon	charge (Mulliken)	spin density	charge (Mulliken)	spin density	charge (Mulliken)	spin density
1	0.25	0.38	0.06	0.02	0.21	0.2
2	0.15	0.16	0.17	0.28	0.08	−0.07
3	0.18	−0.01	0.12	−0.12	0.2	0.17
4	0.25	0.45	0.17	0.29	0.07	0.02
5	0	0	0.12	−0.08	0.1	−0.06
6	0	0	0.25	0.61	0.21	0.73
methyl	0.17	0.04	0.1	0	0.12	0

This strongly suggested that the pathway would not be followed because the structure would prefer to fall back to the ion−molecule complex. To be thorough, the previous scans were completed while freezing the coordinate that changed drastically earlier (usually the C4−C5 bond or the C3−C4−C5−C6 dihedral). The geometries corresponding to the low- and high-energy points in the scan were optimized, while keeping the new constraint frozen.

In the starting material, there is a partial positive charge of +0.20 on C1, while C4 is nearly neutral. This charge increases to +0.23 in transition structure **1a**−**7**•+ and remains approximately the same for intermediate **1a**−**8**•+. Charges and spin densities of the starting materials and intermediates **1a**−**8**•+ and **1b**−**8**•+ can be found in Table 1. The most stable intermediate has large portions of the charge and spin density located on the carbon with the methyl substituent. This trend is general for all of the pathways. Bond formation to C1 faces both steric repulsion and electronic destabilization of the radical/cation. The difference in steric repulsion is only minimal in the anti-intermediate as the shortest distance from a methyl hydrogen to a hydrogen on C5 is only 0.13 Å shorter for **1a**−**8**•+. As the C1−C5 bond is formed, the radical/cation must shift from a disubstituted carbon to a monosubstituted position. The pathways stemming from pathway 1b are strongly favored over those of **1a**•+. The highest point of the four stepwise pathways after bond formation at C4 is the transition structure **1b**−**12**•+, which is 2.4 kcal/mol below the energy of the lowest possible barrier in the pathways that follow from bond formation at C1. Transition structure **1a**−**7**•+ is shifted 4.5 kcal/mol above structure **1b**−**7**•+, while the ion−molecule complexes are less than 1 kcal/mol apart. The **1a**−**7**•+ structure C1−C5 bond length is 0.23 Å shorter than the C4−C5 bond length in **1b**−**7**•+, while the bond is 0.15 Å shorter in **1b**−**8**•+ than in **1a**−**8**•+. These

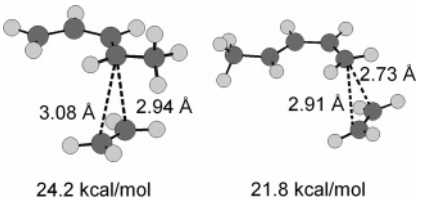

FIGURE 5. Ion−molecule complex structures and relative energies for **2a**−**4**$^{\bullet+}$ and **2b**−**4**$^{\bullet+}$.

substantial differences strongly disfavor the five pathways that follow the 1a attack at the substituted carbon. Only the five pathways that begin with an attack at C4 (1b pathways) need be considered.

Position 2: *trans*-1,3-Pentadiene and Ethylene. The reaction of *trans*-1,3-pentadiene and ethylene is very similar to that of *cis*-1,3-pentadiene and ethylene. There are two different ways in which the two molecules can approach each other: approach where the initial bond in the stepwise pathways is formed between C1 and C5 (pathway 2a), and where the initial bond is formed between C4 and C5 (pathway 2b). Because of the lack of steric repulsion of the endo methyl group and the resulting higher stability of *trans*-penta-1,3-diene, the separated starting materials are 29 kcal/mol in energy above the lowest energy conformation of the product 3-methyl-cyclohexene. The differentiation between the two main approaches begins at the ion−molecule complexes **2a**−**4**$^{\bullet+}$ and **2b**−**4**$^{\bullet+}$ shown in Figure 5, where the differences in bond lengths follow the same pattern as that in **1a**−**4**$^{\bullet+}$ and **1b**−**4**$^{\bullet+}$. Pathway 2a that forms the initial bond to C1 in the starting material again faces electronic and steric destabilization when compared to pathway 2b. Electronic destabilization comes from having to move the radical/cation from C1, which is only necessary if a bond forms there. However, it is noteworthy that the energy difference between **2a**−**4**$^{\bullet+}$ and **2b**−**4**$^{\bullet+}$ is 2.4 kcal/mol, significantly larger than in the earlier case, which is most likely due to the fact that the ethylene moiety in **2b**−**4**$^{\bullet+}$ is not subject to steric repulsion by an endo methyl group. Similarly, the energies of the transition structure leading to the anti-intermediate are 30 kcal/mol for **2a**−**7**$^{\bullet+}$ and 23.5 kcal/mol for **2b**−**7**$^{\bullet+}$. Anti-intermediate **2a**−**8**$^{\bullet+}$ has an energy of 30.2 kcal/mol, and **2b**−**8**$^{\bullet+}$ is at 20.9 kcal/mol relative to the product. This additional steric repulsion in pathway 2a as compared to 2b puts the highest energy transition structure of the stepwise pathways of 2b (24.8 kcal/mol for transition structure **2b**−**12**) 5.2 kcal/mol below the energy of the lowest possible barrier in the 2a pathways. The attack at the more highly substituted position is therefore energetically disfavored and not likely to occur.

Energies of the structures in the five pathways from approach 2b are shown in Figure 6. The transition structure for the concerted pathway **2b**−**6**$^{\bullet+}$ could again only be located by constraining the two forming bonds to be equal and has two negative eigenvalues. It is 14.2 kcal/mol higher in energy than the starting materials and even further above all the rest of the other structures, again ruling out the concerted pathway. The barrier for the formation of the anti-intermediate **2b**−**8**$^{\bullet+}$ is 1 kcal/mol lower in energy than the barrier for the gauche-out intermediate **2b**−**11**$^{\bullet+}$, close to the error limits of the method used here. The two intermediates are again easily interconvertible and can close down to *trans*-propenyl-cyclobutane **2b**−**14**$^{\bullet+}$, or close down to the 3-methylcyclohexene radical cation with an activation energy of 1.6 kcal/mol. The transition state for the formation of the cyclobutane ring, **2b**−**12**$^{\bullet+}$, is 1.7 kcal/mol above the one for the interconversion, **2b**−**13**$^{\bullet+}$, and 2.3 kcal/mol above the barrier to close down to the six-membered ring from the anti-intermediate via **2b**−**9**$^{\bullet+}$. For these reasons, the anti and gauche to anti pathways that eventually form the 3-methylcyclohexene radical cation are significantly favored over the two that proceed to form a butane ring. The anti pathway is the most favored pathway because of the lower energy for the formation of intermediate **2b**−**8**$^{\bullet+}$ from the ion−molecule complex.

Figure 7 shows the geometries of the rate-determining transition structures **2b**−**12**$^{\bullet+}$ and **2b**−**9**$^{\bullet+}$ for the vinylcyclobutane and cyclohexene formation, respectively. It can be seen that the calculated bond lengths for the forming bonds are with 2.93 and 4.35 Å, respectively, very long. It is therefore clear that the origin of the barrier is mostly in the eclipsed conformation around the C4−C5 bond. This is consistent with the fact that the barriers for this rotation are 1.4 kcal/mol higher in the 2a pathway (see the Supporting Information).

Position 3: 1,3-Butadiene and 1-Propene. With the starting materials 1,3-butadiene and 1-propene, reaction can occur at either the more (pathway a) or the less substituted (pathway b) of the vinylic carbons to form a bond with the diene in a stepwise fashion. Approach can also occur with the methyl group pointing toward either the inside (endo) or the outside (exo) of the diene. In all four possible approaches, stationary points corresponding to the ion−molecule complexes could not be located. The formation of the anti and gauche-out intermediates for both pathways 3be and 3bx were found to be barrierless (see scans in the Supporting Information). The energies of the

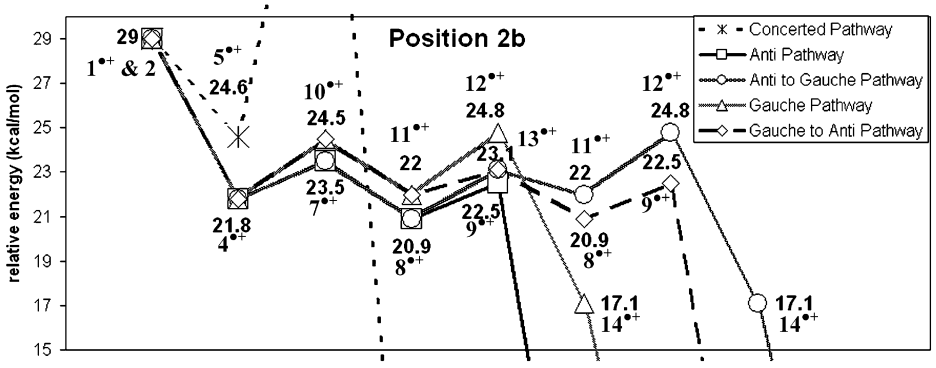

FIGURE 6. Calculated reaction profiles for reaction 2b. Second-order transition structure at 43.2 kcal/mol and the cyclohexene product at 0 kcal/mol are not shown.

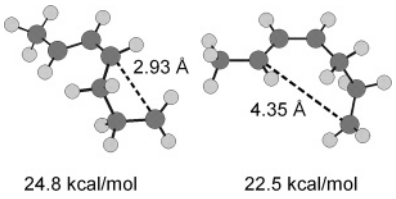

FIGURE 7. Transition structures and relative energies for **2b**−**12**$^{\bullet+}$ and **2b**−**9**$^{\bullet+}$.

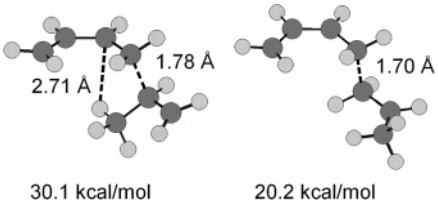

FIGURE 8. Calculated structures and relative energies for **3ae**−**8**$^{\bullet+}$ and **3be**−**8**$^{\bullet+}$.

anti-intermediates relative to 4-methylcyclohexene are 30.1 kcal/mol for **3ae**−**8**$^{\bullet+}$, 29.8 kcal/mol for **3ax**−**8**$^{\bullet+}$, 20.2 kcal/mol for **3be**−**8**$^{\bullet+}$, and 19.9 kcal/mol for **3bx**−**8**$^{\bullet+}$. The structures **3ae**−**8**$^{\bullet+}$ and **3be**−**8**$^{\bullet+}$ are shown in Figure 8.

The lowest barrier resulting from any of the eight pathways involving attack at C5 (pathways 3a) is 29.8 kcal/mol relative to the product. While the transition structure **3bo**−**12**$^{\bullet+}$ is only 1.3 kcal/mol below this, all other barriers in the 3b pathways are 5−7 kcal/mol lower. Similar to the cases discussed earlier, initial bond formation between C5 and C1 causes a strong steric repulsion between the methyl group and C2 or the hydrogen on C2. It also prevents the radical/cation from being placed on the more highly substituted C5. The stabilization obtained by placing the radical/cation on C5 is so strong that the formation of the 3b anti and gauche-out intermediates **3b**−**8**$^{\bullet+}$ and **3b**−**11**$^{\bullet+}$ from both endo and exo attacks is barrierless from the starting materials, as shown in Figure 9.[14] All 3a pathways are therefore ruled out for energetic reasons. The two possible concerted pathways involving second-order transition structures **3e**−**6**$^{\bullet+}$ and **3x**−**6**$^{\bullet+}$, located again under constraints, are also energetically not viable because the concerted transition structures are more than 14 kcal/mol above the 3b pathways. The eight remaining pathways can be seen in Figure 9.

The 3b pathways that remain after exclusion of the unfavorable concerted and 3a pathways are energetically very close. The two remaining endo and exo approaches yield very similar results in terms of the relative energies because they both provide a similar stabilization of the radical/cation and the methyl group has very little steric interaction with the rest of the molecule. The pathway with the lowest barrier in both cases is the anti pathway with a negligible difference in energy of 0.1 kcal/mol between the higher energy endo and exo transition states **3be**−**9**$^{\bullet+}$ and **3bx**−**9**$^{\bullet+}$ with relative energies of 22.0 and 22.1 kcal/mol, respectively. The energy difference between the endo and exo orientations for the two pathways is less than 0.5 kcal/mol. With relative energies of 22.4 kcal/mol for **3bx**−**13**$^{\bullet+}$ and 22.6 kcal/mol for **3be**−**13**$^{\bullet+}$, both pathways will participate in the overall reaction to a significant degree. Each of the other stepwise pathways (gauche-out via **3b**−**12**$^{\bullet+}$ and anti-to-gauche via **3b**−**13**$^{\bullet+}$) form the 1-methyl-2-vinyl-cyclobutane product. As was the case in the reactions discussed earlier, the highest point in these pathways is the transition state for the formation of the cyclobutane ring. As the C2−C5 bond forms, there is a counterclockwise rotation about the C5−C6 bond. This positions the methyl group in transition structure **3bx**−**12**$^{\bullet+}$ toward the hydrogen atoms on C1 and C2, as shown in Figure 10. The added steric repulsion increases the energy of **3bx**−**12**$^{\bullet+}$ by 3.9 kcal/mol over **3be**−**12**$^{\bullet+}$. The gauche and anti-to-gauche pathways from the 3bx approach are both strongly disfavored by this large barrier. These pathways in the 3be approach may have only a minor contribution to the overall product distribution as their barrier is 2−2.6 kcal/mol above the highest energy structures in the anti and gauche to anti pathways. The highest barriers in the anti and gauche to anti pathways are all within

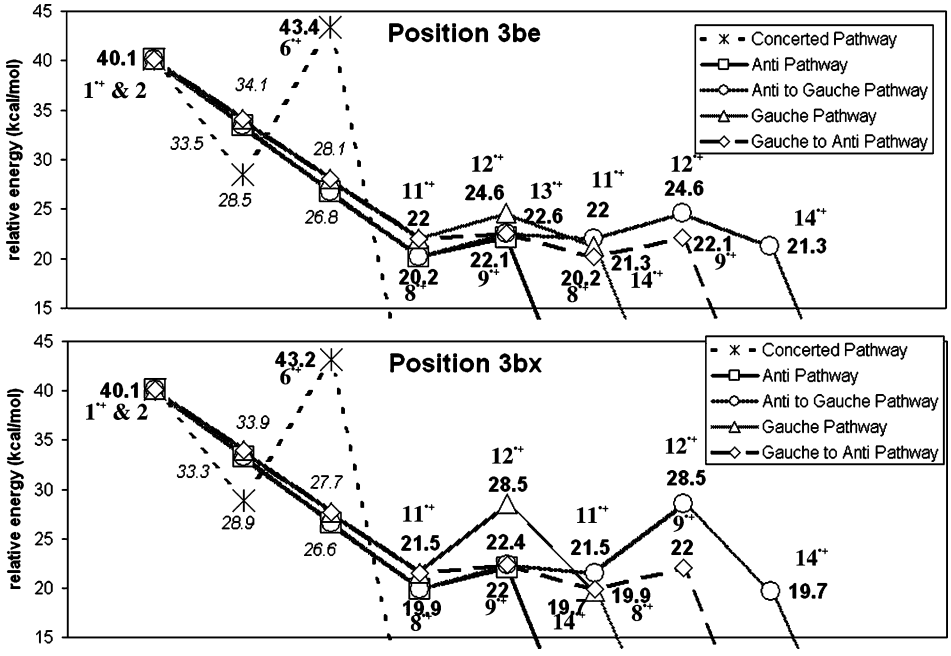

FIGURE 9. Calculated reaction profiles for reactions 3be and 3bx. Cyclohexene products at 0 kcal/mol are not shown. Points in italics are not stationary points.

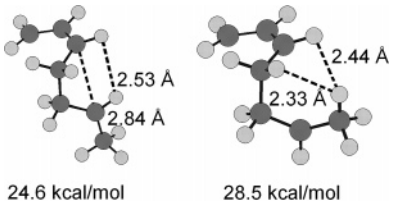

FIGURE 10. Transition structures and relative energies for **3be**−**12**$^{\bullet+}$ and **3bx**−**12**$^{\bullet+}$.

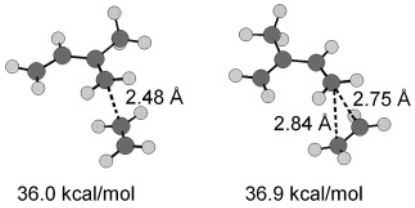

FIGURE 11. Ion−molecule complex structures and relative energies for **4a**−**4**$^{\bullet+}$ and **4b**−**4**$^{\bullet+}$.

0.6 kcal/mol of each other, with the two anti pathways being the lowest by about 0.5 kcal/mol. Both of these pathways for each approach can be expected to have a significant contribution to the mechanism, and all of them lead directly to the formation of 4-methyl-1-cyclohexene. This is in agreement with the experimentally observed low endo/exo selectivity of the radical cation Diels−Alder reaction, which is in the range of 1:1 to 3:1 and therefore much smaller than the observed regio- and diastereoselectivity.[8,9]

Position 4: 2-Methyl-1,3-butadiene and Ethylene. The two approaches at either C1 or C4 for the reaction of 2-methyl-1,3-butadiene and ethylene lead to the two ion−molecule complexes **4a**−**4**$^{\bullet+}$ and **4b**−**4**$^{\bullet+}$, respectively. The stabilization energy of these ion−molecule complexes, shown in Figure 11, is with 8.6 and 7.7 kcal/mol slightly higher than was the case for the penta-1,3-dienes. This, together with the higher overall exothermicity, indicates that the methyl group in 2-position stabilizes the butadiene radical cation less than in the 1-position.

While the preference for attack at C1 at the stage of the ion−molecule complex is 0.9 kcal/mol, within the error limits of the method used here, the energy differences between the two approaches again increase significantly once the initial bonds are formed. For example, the anti-intermediates with relative energies of 32.8 kcal/mol for **4a**−**8**$^{\bullet+}$ and 38.4 kcal/mol for **4b**−**8**$^{\bullet+}$ are formed via transition structures **4a**−**7**$^{\bullet+}$ and **4b**−**7**$^{\bullet+}$ with relative energies of 36.1 and 39.1 kcal/mol, respectively. Closure of the anti-intermediate to form methylcyclohexene requires 34.4 kcal/mol for the 4a pathways and 39.8 kcal/mol for the 4b pathways. The gauche-out intermediates, **4a**−**11**$^{\bullet+}$ with energy 32.1 kcal/mol and **4b**−**11**$^{\bullet+}$ at 40 kcal/mol, can also be formed from the initial ion−molecule complexes. Similarly, formation of the gauche-out intermediate from the ion−molecule complex proceeds through transition structures **4a**−**10**$^{\bullet+}$ and **4b**−**10**$^{\bullet+}$ with relative energies of 36.8 and 40.5 kcal/mol, respectively. These fairly large energy differences effectively eliminate attack at C4 as a viable mechanistic pathway. The five different possible pathways derived from the more favorable attack at C1 (pathways 4a) are summarized in Figure 12.

It is interesting to note that, while the concerted pathway could, as in the earlier examples, only be located by constraining the two forming bonds to be of equal length, and the corresponding transition structure is still 8.3 kcal/mol uphill from the reactants and is therefore energetically not feasible, **4a**−**6**$^{\bullet+}$ is a true transition structure with one imaginary frequency. Unlike its counterparts in the other three reactions studied here, it is therefore not subject to the Jahn−Teller distortion.

The low-energy stepwise pathways are quite comparable to those obtained from the other substitution patterns. The activation energies for the formation of the 1-methyl cyclohexene radical cation via **4a**−**9**$^{\bullet+}$ and the anti-gauche isomerization **4a**−**13**$^{\bullet+}$, within approximately 2 kcal/mol, are essentially identical. However, the formation of the vinyl cyclobutane radical cation is energetically prohibitive because of the unusually high energy of the ring-closing transition structure **4a**−**12**$^{\bullet+}$ with a relative energy of 37.2 kcal/mol. This is due to the steric repulsion in the transition structure leading to the formation of a quaternary center that can also be seen in the structure of **4a**−**14**$^{\bullet+}$ shown in Figure 13. This finding is in agreement with the experimentally observed difficulty of bond formation to highly substituted carbons in radical cation Diels−Alder reactions.[1a,8,9] The transition state for formation of the gauche-out intermediate **4b**−**10**$^{\bullet+}$ is only 0.7 kcal/mol above the one for the formation of the anti-intermediate, **4b**−**7**$^{\bullet+}$. Another interesting feature in this pathway is the fact that the energy of the gauche intermediate **4a**−**11**$^{\bullet+}$ is 0.7 kcal/mol below the energy of intermediate **4a**−**8**$^{\bullet+}$. This phenomenon does not occur in any of the other cases and may be explained by an agostic interaction between C6 and a hydrogen on the methyl group, as shown in Figure 13. This attractive interaction is not present in any of the other

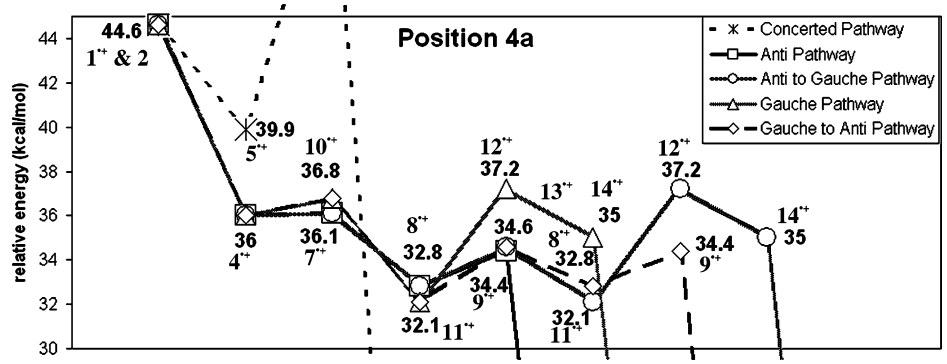

FIGURE 12. Calculated reaction profiles for reaction 4a. Constrained transition structure at 52.9 kcal/mol and the cyclohexene product at 0 kcal/mol are not shown.

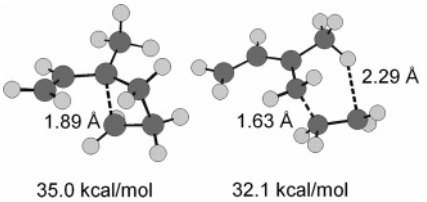

FIGURE 13. Structures and relative energies of methyl vinyl cyclobutane **4a**−**14**$^{\bullet+}$ and gauche-out intermediate **4a**−**11**$^{\bullet+}$.

intermediates or in ion−molecule complex **4a**−**4** and accounts for differences in the relative energy of the two intermediates in this case.

Conclusions

Substitution of the diene and dienophile of the parent radical cation Diels−Alder reaction by a single methyl group leads to four different substitution patterns. A concerted pathway could only be located by constraining the pathway and proceeds in all but one case through a second-order transition structure. Although the symmetry of the reaction is formally broken, the concerted mechanism is prohibitively high in energy, and all but one of the transition structures have two negative eigenvalues due to Jahn−Teller distortions. This is in line with the notion that cyclic conjugated odd-electron systems are destabilized by antiaromaticity,[15] as well as the experience that, for neutral pericyclic reactions, the results of the orbital symmetry analysis are still transferable to non-symmetric substrates. Upon release of the constraints, the concerted pathway follows the symmetry-breaking, strong negative eigenfrequency to form one of the species involved in the stepwise pathways.

In the remaining four stepwise pathways, attack at the less substituted carbon is favored for both isomers of 1,3-pentadiene as well as propene due to the formation of the more stable acyclic intermediate. The reaction of the 2-methyl butadiene radical cation occurs preferentially by initial bond formation at C1. It shows some notable differences from the other pathways in that the transition structure to formation of the cyclobutane ring in the gauche pathway is relatively high in energy. The anti pathway leading to the formation of the cyclohexene product is generally favored, but the substitution pattern has a significant impact on the energy difference between the gauche and the anti pathways.

The results presented here emphasize the differences from and similarities to the only other pericyclic radical cation reaction for which substituent effects have been systematically studied, the ring opening of 3-substituted cyclobutenes. Whereas a concerted, non-symmetric pathway was found to be energetically favored this reaction was favored for all substituents, and the stepwise anti-pathway was found to be preferred in the present study. These results are in line with the findings for the corresponding parent cases and indicate that many of the results from simple model studies can be transferred to more complex reactants. Future studies will have to investigate whether these findings hold true for substituents with stronger electronic effects than the methyl group studied here and uncover the origin of the preferred formation and subsequent rearrangement of the vinylcyclobutane radical cation, the so-called "indirect Diels−Alder reaction", in some heterosubstituted cases.[11]

Acknowledgment. We thank the Center for Research Computing at the University of Notre Dame for the generous allocation of computing resources and the National Science Foundation (Grant No. CHE-0415344 to O.W.) for financial support.

Supporting Information Available: Energies, geometries, and imaginary frequencies of all stationary points as well as scans completed for non-stationary points. This material is available free of charge via the Internet at http://pubs.acs.org.

JO0620361

(14) This case differs from the previously studied radical cation Diels−Alder reaction of the indole radical cation as a highly stabilized dienophile radical cation. In this reaction, the ion−molecule complex can be located, cf., ref 9b.

(15) Allen, A. D.; Tidwell, T. T. *Chem. Rev.* **2001**, *101*, 1333−1348.